

## Self-consistent density of states for a single- and double-quantum-well structure in a parallel magnetic field

Godfrey Gumbs\*

*Department of Physics and Astronomy, Hunter College of the City University of New York, 695 Park Avenue, New York, New York 10021*

(Received 5 February 1996; revised manuscript received 8 July 1996)

The electron energy eigenstates for an isolated and a pair of strongly coupled quantum-well structures with a quantizing magnetic field  $B_{\parallel}$  parallel to the planes are calculated. Numerical results are presented for the energy eigenvalues as a function of  $B_{\parallel}$  as well as the in-plane wave number  $k_y$ . The results show a crossover behavior as the magnetic field is increased, with the critical magnetic field corresponding to the well width being equal to the magnetic length. This implies that for the pair of coupled quantum wells the tunneling between wells is suppressed in the high magnetic field regime with the electrons confined to the wells, which is also evident from the wave functions. In the low magnetic field regime, the energy eigenvalue spectrum is more densely distributed compared to the high magnetic field region. When plotted as a function of  $k_y$ , the energy spectra for both the single- and double-quantum-well systems have gaps. The eigenfunctions for the lowest states are also presented for  $k_y=0$  and  $k_y$  finite to demonstrate their dependence on this wave vector. These results are used to obtain the partial density of states for each energy eigenvalue as a function of the electron energy for fixed magnetic field strength. The role played by impurity scattering is included in the self-energy, through the self-consistent Born approximation. The magnitude of the contribution from the self-energy to the partial density of states increases with the magnetic field. The role played by the electron tunneling between coupled wells for the self-consistent density of states is included. [S0163-1829(96)06740-9]

### I. INTRODUCTION

Recently, there has been a considerable amount of interest in strongly coupled two-dimensional electron gas (2DEG) systems.<sup>1-5</sup> In a double-quantum-well (DQW) structure, the tunneling between the two parallel 2DEG layers introduces several interesting features in the cyclotron resonance, magnetoplasmon excitation spectrum, as well as the electrical transport, all of which have no counterpart in a single 2DEG. The effect due to tunneling could of course be adjusted by varying the thickness of the barrier layer separating the two quantum wells (QW's). As reported recently, the role of tunneling has also been demonstrated in theoretical calculations of the magnetoplasmon excitation for a magnetic field perpendicular to the 2DEG layers.<sup>6</sup> In a series of papers, Simmons *et al.*<sup>7-9</sup> and Lyo<sup>10,11</sup> have reported on experiments for the conductivity and cyclotron resonance for DQW structures when a magnetic field is applied parallel to the 2D planes. In Ref. 8, the magnetic field  $B_{\parallel}$  is in the  $z$  direction, the electron gases are in the  $y$ - $z$  plane, and the electric field  $\vec{E}$  makes an angle  $\theta$  with  $B_{\parallel}$ . The component of the current  $\vec{j}$  in the direction of  $\vec{E}$  yields the in-plane magnetoconductivity  $\vec{j} \cdot \vec{E}/E^2$  which exhibits several interesting features due to magnetic field-induced anticrossing of the electron energy bands.

In this paper, we are interested in calculating the single-electron wave functions, the energy eigenvalues, and their density of states for a single quantum well and a pair of coupled quantum wells,<sup>4,12</sup> in the presence of a magnetic field parallel to the planes confining the electron gases. For a pair of coupled QWs, the quadratic energy dispersions of electrons in a single well anticross due to the in-plane mag-

netic field and the tunneling in the DQW structure. This will produce minigaps and saddle points in the density of states when  $B_{\parallel}$  is strong. Our results for the energy eigenvalues as a function of  $B_{\parallel}$  show the splitting of the originally degenerate Landau energy levels due to tunneling in the strong magnetic field limit. The partial density of states is obtained using the self-consistent Born approximation. The role played by the impurity interaction matrix element increases with the magnetic field. Therefore, the self-consistency of the calculation for the density of states becomes more important in the high magnetic field regime. This is the first step in a calculation of the static conductivity  $\sigma_{\perp}$  for a quantum-well structure in the presence of an in-plane magnetic field with the electric field and the current along the growth  $x$  axis. Resonant tunneling experiments have also been reported for DQWs in a parallel magnetic field.<sup>13-15</sup> These experiments show the effect due to tunneling on the current-voltage characteristics. The results of the present paper could be applied in analyzing the results of these experiments.

The outline of the rest of this paper is as follows. In Sec. II, we derive the dispersion relation for the energy eigenvalues and eigenfunctions of a single quantum well in a magnetic field  $B_{\parallel}$  parallel to the confining potential. Detailed numerical results are given for the eigenvalue spectrum as a function of  $B_{\parallel}$  and the wave vector dispersion for the in-plane wave vector for a fixed value of the magnetic field strength. In Sec. III, we repeat the calculations of Sec. II for a pair of strongly coupled quantum wells. In Sec. IV, we formulate the calculation of the density of states in the self-consistent Born approximation and provide numerical results for the single- and double-quantum-well structures. Section V contains a summary of our results and some conclud-

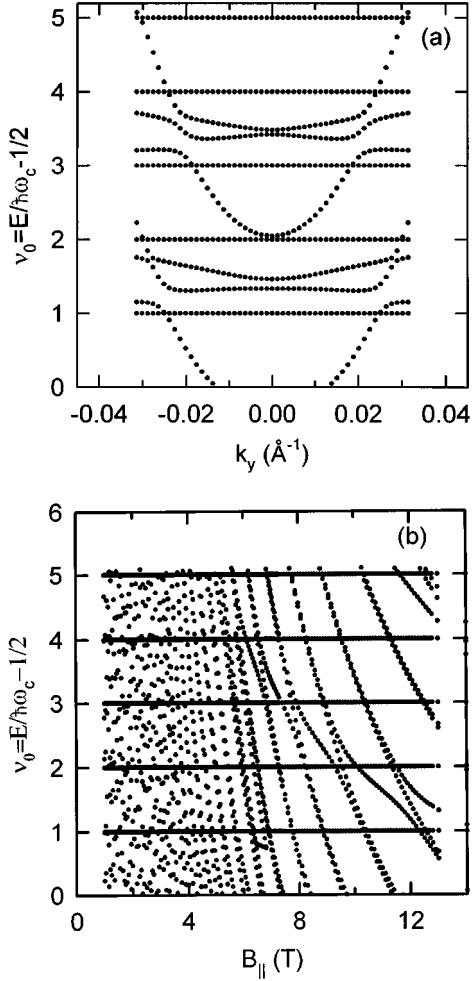


FIG. 1. Plot of the lowest scaled energy eigenvalues  $\nu_0 = E_j(k_y)/\hbar\omega_c - 1/2$  for a single quantum well. We chose  $m^* = 0.0667m_e$ ,  $U_0 = 213$  meV, and  $2a = 200$  Å. In (a),  $\nu_0$  is plotted as a function of  $k_y$  in the unit of Å<sup>-1</sup> for  $B_{\parallel} = 10$  T. In (b),  $\nu_0$  is plotted as a function of  $B_{\parallel}$  for  $k_y = 0$ . The Landau levels are at integer values.

ing remarks. An Appendix is devoted to some mathematical details for the parabolic cylinder function, in terms of which the eigenfunctions are expressed.

## II. SINGLE-PARTICLE EIGENSTATES FOR A SINGLE QUANTUM WELL

Let us first consider electrons moving in the  $y$ - $z$  plane in a magnetic field  $B_{\parallel}$  parallel to the  $z$  axis and a one-dimensional potential  $U_{\text{ext}}(x)$ . In the Landau gauge with vector potential  $\vec{A} = (0, B_{\parallel}x, 0)$ , the Schrödinger equation for an electron has the form

$$\left[ -\frac{\hbar^2}{2m^*} \frac{\partial^2}{\partial x^2} - \frac{\hbar^2}{2m^*} \frac{\partial^2}{\partial z^2} + \frac{1}{2m^*} \left( -i\hbar \frac{\partial}{\partial y} + eB_{\parallel}x \right)^2 + U_{\text{ext}}(x) \right] \psi_{j\vec{k}_{\parallel}}(\vec{r}) = E_j(\vec{k}_{\parallel}) \psi_{j\vec{k}_{\parallel}}(\vec{r}), \quad (1)$$

and, for simplicity, the spatial variation of the electron effective mass in the well and barrier regions is accounted for by

using the average value  $m^*$  in Eq. (1). Here  $j$  is a quantum number labeling the subbands and  $\vec{k}_{\parallel} = (k_y, k_z)$ . We note that for a symmetric potential with  $U_{\text{ext}}(-x) = U_{\text{ext}}(x)$ , the Hamiltonian in this gauge is invariant under  $B_{\parallel}$  to  $-B_{\parallel}$  when we make the replacement  $x \rightarrow -x$ . For Eq. (1), we write the wave function in the form of  $\psi_{j\vec{k}_{\parallel}}(\vec{r}) = \phi_{jk_y}(x) \exp(ik_y y + ik_z z) / \sqrt{A}$ , where  $A$  is the cross-sectional area of the 2DEG, and we introduce a new variable  $\xi_{k_y} = \sqrt{2}(x/\ell_H + \ell_H k_y)$ . Then, Eq. (1) yields

$$\frac{\partial^2 \phi_{jk_y}(\xi_{k_y})}{\partial \xi_{k_y}^2} + \left[ \frac{E_j(k_y) - U_{\text{ext}}(\xi_{k_y})}{\hbar\omega_c} - \frac{\xi_{k_y}^2}{4} \right] \phi_{jk_y}(\xi_{k_y}) = 0, \quad (2)$$

where  $E_j(k_y) = E_j(\vec{k}_{\parallel}) - \hbar^2 k_z^2 / 2m^*$ ,  $\omega_c = eB_{\parallel} / m^*$ ,  $\ell_H = \sqrt{\hbar / eB_{\parallel}}$  is the magnetic length, and  $U_{\text{ext}}$  stands for the potential of a single well (or a DQW in the next section). Thus the electron potential in Eq. (2) consists of a square well potential that is symmetric about  $x = 0$  and a magnetic parabola with its minimum at  $x = -k_y \ell_H^2$ . We note that when  $U_{\text{ext}}$  in Eq. (2) is a constant, we have the standard equation for parabolic cylinder functions. Subsequently, for the QW structures we consider, the general solution of Eq. (2) can be expressed in terms of two linearly independent parabolic cylinder functions  $D_{\nu}(\xi_{k_y})$  and  $V_{\nu}(\xi_{k_y})$ , where  $\nu = [E_j(k_y) - E_0] / \hbar\omega_c - 1/2$ , with  $E_0 = 0$  or  $U_0$  in the well or barrier region, respectively. For convenience, we have given integral representations of these special functions in the Appendix, which are used in our numerical calculations. These functions have the following properties:<sup>16</sup>

$$D_{\nu}(\xi_{k_y}) = \begin{cases} 0, & \xi_{k_y} \rightarrow \infty \\ \infty, & \xi_{k_y} \rightarrow -\infty, \end{cases} \quad (3)$$

$$V_{\nu}(\xi_{k_y}) = \begin{cases} \infty, & \xi_{k_y} \rightarrow \infty \\ 0, & \xi_{k_y} \rightarrow -\infty, \end{cases} \quad (4)$$

whose linear combination can be used to construct the general solution of Eq. (1).

For a single quantum well, the solution inside the well,  $-a < x < a$ , is

$$\phi_{jk_y}(x) = C_j^{(2)}(k_y) D_{\nu_0}(\xi_{k_y}) + C_j^{(3)}(k_y) V_{\nu_0}(\xi_{k_y}), \quad (5)$$

where  $\nu_0 = E_j(k_y) / \hbar\omega_c - 1/2$  and, similarly, the solution in the two barrier regions can be written as

$$\phi_{jk_y}(x) = \begin{cases} C_j^{(1)}(k_y) V_{\nu_1}(\xi_{k_y}), & x < -a \\ C_j^{(4)}(k_y) D_{\nu_1}(\xi_{k_y}), & x > a, \end{cases} \quad (6)$$

where  $\nu_1 = [E_j(k_y) - U_0] / \hbar\omega_c - 1/2$ . In terms of the continuous boundary conditions for the wave functions and their derivatives, we obtain the following equation determining  $E_j(k_y)$  and  $C_j^{(i)}(k_y)$ :

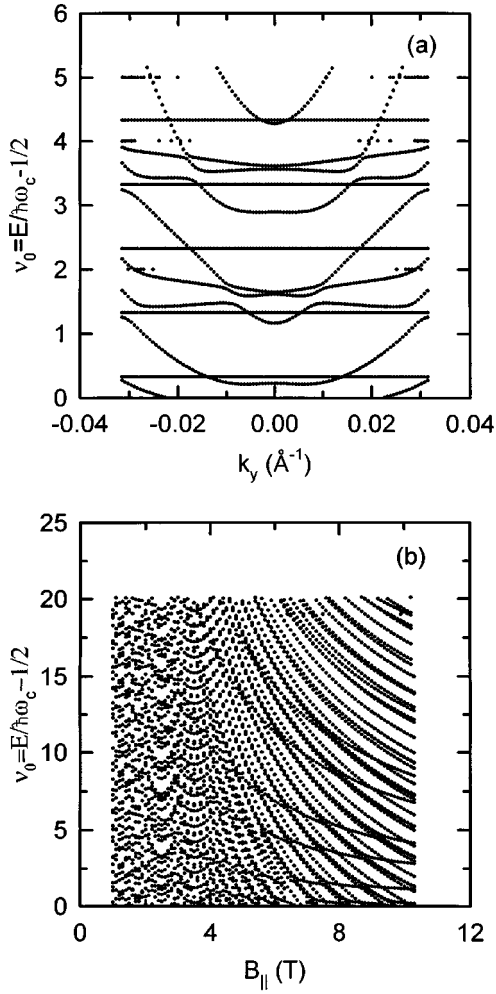


FIG. 2. Plot of the lowest scaled energy eigenvalues  $\nu_0 = E_j(k_y)/\hbar\omega_c - 1/2$  for a double quantum well. We chose  $m^* = 0.0667m_e$ ,  $U_0 = 213$  meV,  $2a = 200$  Å, and the barrier separating the two wells has width  $b = 20$  Å. In (a),  $\nu_0$  is plotted as a function of  $k_y$ , in the unit of Å<sup>-1</sup> for  $B_{\parallel} = 10$  T. In (b),  $\nu_0$  is plotted as a function of  $B_{\parallel}$  for  $k_y = 0$ .

$$\begin{pmatrix} \tilde{V}_{\nu_1}(-a) & -\tilde{D}_{\nu_0}(-a) & -\tilde{V}_{\nu_0}(-a) & 0 \\ \tilde{V}'_{\nu_1}(-a) & -\tilde{D}'_{\nu_0}(-a) & -\tilde{V}'_{\nu_0}(-a) & 0 \\ 0 & -\tilde{D}_{\nu_0}(a) & -\tilde{V}_{\nu_0}(a) & \tilde{D}_{\nu_1}(a) \\ 0 & -\tilde{D}'_{\nu_0}(a) & -\tilde{V}'_{\nu_0}(a) & \tilde{D}'_{\nu_1}(a) \end{pmatrix} \times \begin{pmatrix} C_j^{(1)}(k_y) \\ C_j^{(2)}(k_y) \\ C_j^{(3)}(k_y) \\ C_j^{(4)}(k_y) \end{pmatrix} = 0, \quad (7)$$

where, for convenience, we have introduced the following notations:

$$\tilde{D}_{\nu_0}(x) \equiv D_{\nu_0}(\xi_{k_y}), \quad \tilde{V}_{\nu_0}(x) \equiv V_{\nu_0}(\xi_{k_y}), \quad (8a)$$

$$\tilde{D}'_{\nu_0}(x) \equiv \frac{d\tilde{D}_{\nu_0}(\xi_{k_y})}{d\xi_{k_y}}, \quad \tilde{V}'_{\nu_0}(x) \equiv \frac{d\tilde{V}_{\nu_0}(\xi_{k_y})}{d\xi_{k_y}}. \quad (8b)$$

From Eq. (7), we can express  $C_j^{(2)}(k_y), \dots, C_j^{(4)}(k_y)$  in terms of  $C_j^{(1)}(k_y)$  which must itself be determined from the normalization condition for each eigenstate wave function  $\phi_{jk_y}(x)$  given by Eqs. (5) and (6).

In Fig. 1(a), we present results for the scaled energy eigenvalues  $\nu_0 = E_j(k_y)/\hbar\omega_c - 1/2$  in a single quantum well, obtained by solving Eq. (7) as a function of  $k_y$  for a parallel magnetic field  $B_{\parallel} = 10$  T. Here, we take  $m^* = 0.067m_e$ , where  $m_e$  is the free-electron mass,  $2a = 200$  Å, and  $U_0 = 213$  meV. For these values of  $B_{\parallel}$  and  $m^*$ ,  $\hbar\omega_c = 17.264$  meV so that all the levels shown lie below the top of the potential barrier. These calculations show that when the homogeneous 2DEG is modulated by a single-square-well potential, the  $k_y^2$ -dispersion relation for each quantized energy level in the absence of an external magnetic field becomes hybridized with each of the originally degenerate Landau levels of a homogeneous 2DEG in the presence of an external magnetic field, which are independent of  $k_y$ . The results in Fig. 1(a) show that the  $k_y$  dispersion may vary from one energy level to another and that the effects due to scattering from the quantum well are largest for the high energy states whose orbital radii increase with the Landau level index. Thus the electron motion in the well does not follow the guiding center and the spacing between energy levels is not constant. In Fig. 1(a), we also show the Landau levels for the homogeneous 2DEG, which are straight lines at integer values parallel to the  $k_y$  axis when the energy levels are scaled by  $\hbar\omega_c$  and 1/2 is subtracted from the result. In Fig. 1(b), we display the energy eigenvalues in a single quantum well as a function of the parallel magnetic field  $B_{\parallel}$ . Here, we take  $\tilde{k}_{\parallel} = 0$ , and all the other parameters for the quantum well, i.e., the well width, the barrier height, and the electron effective mass, are the same as Fig. 1(a). In the low magnetic field regime, there is considerable mixing of the Landau orbits from different Landau levels and with different guiding centers due to the presence of the potential barriers. This results in the densely distributed energy eigenvalues at low magnetic field. As the magnetic field is increased, the orbits become commensurate with the width of the well ( $l_H = a$  when  $B_{\parallel} \sim 6.6$  T). At large magnetic fields where the diameter of the orbits is much less than the well width, the mixing of the Landau levels and Landau orbits for the electrons by the confining potential is negligible, thereby giving rise to the approaching of the energy levels to Landau levels. The separation between the energy levels within the well in the absence of a magnetic field increases with energy whereas the energy levels within the magnetic parabola are equally spaced. However, as the magnetic field is increased, the curvature of the magnetic parabola increases and the energy levels are shifted upwards. Therefore, when the  $\hbar\omega_c$  factor is included in the energy diagram of Fig. 1(b) the energy eigenvalues increase with the magnetic field.

### III. SINGLE-PARTICLE EIGENSTATES FOR A DOUBLE QUANTUM WELL

For the DQW structure where each well has width  $2a$  and the barrier between them is  $-b/2 < x < b/2$ , we have in the

first region ( $x < x_1$ ) a barrier with  $E_0 = U_0$ , in the second region ( $x_1 < x < x_2$ ) a quantum well with  $E_0 = 0$ , in the third region ( $x_2 < x < x_3$ ) a potential barrier with  $E_0 = U_0$ , in the fourth region ( $x_3 < x < x_4$ ) a quantum well with  $E_0 = 0$ , and in the fifth region ( $x > x_4$ ) a barrier with  $E_0 = U_0$ . Here,

$x_1 = -(2a + b/2)$ ,  $x_2 = -b/2$ ,  $x_3 = b/2$ , and  $x_4 = (2a + b/2)$ . Therefore, we obtain the eigenvalue equation determining  $E_j(k_y)$  from the continuity boundary conditions of the wave functions and their derivatives as

$$\begin{vmatrix} \tilde{V}_{\nu_1}(x_1) & -\tilde{D}_{\nu_0}(x_1) & -\tilde{V}_{\nu_0}(x_1) & 0 & 0 & 0 & 0 & 0 \\ \tilde{V}'_{\nu_1}(x_1) & -\tilde{D}'_{\nu_0}(x_1) & -\tilde{V}'_{\nu_0}(x_1) & 0 & 0 & 0 & 0 & 0 \\ 0 & \tilde{D}_{\nu_0}(x_2) & \tilde{V}_{\nu_0}(x_2) & -\tilde{D}_{\nu_1}(x_2) & -\tilde{V}_{\nu_1}(x_2) & 0 & 0 & 0 \\ 0 & \tilde{D}'_{\nu_0}(x_2) & \tilde{V}'_{\nu_0}(x_2) & -\tilde{D}'_{\nu_1}(x_2) & -\tilde{V}'_{\nu_1}(x_2) & 0 & 0 & 0 \\ 0 & 0 & 0 & \tilde{D}_{\nu_1}(x_3) & \tilde{V}_{\nu_1}(x_3) & -\tilde{D}_{\nu_0}(x_3) & -\tilde{V}_{\nu_0}(x_3) & 0 \\ 0 & 0 & 0 & \tilde{D}'_{\nu_1}(x_3) & \tilde{V}'_{\nu_1}(x_3) & -\tilde{D}'_{\nu_0}(x_3) & -\tilde{V}'_{\nu_0}(x_3) & 0 \\ 0 & 0 & 0 & 0 & 0 & -\tilde{D}_{\nu_0}(x_4) & -\tilde{V}_{\nu_0}(x_4) & \tilde{D}_{\nu_1}(x_4) \\ 0 & 0 & 0 & 0 & 0 & -\tilde{D}'_{\nu_0}(x_4) & -\tilde{V}'_{\nu_0}(x_4) & \tilde{D}'_{\nu_1}(x_4) \end{vmatrix} = 0. \quad (9)$$

From Eq. (9), we can write out  $C_j^{(2)}(k_y), \dots, C_j^{(8)}(k_y)$  in terms of  $C_j^{(1)}(k_y)$ , which in turn has to be obtained from the normalization condition for each wave function  $\phi_{jk_y}(x)$  of the eigenstate.

In Figs. 2(a) and 2(b), we plot the scaled energy eigenvalues  $\nu_0 = E_j(k_y)/\hbar\omega_c - 1/2$  for a pair of strongly coupled QWs. The solutions were obtained by solving Eq. (9) numerically as a function of the in-plane wave vector  $\vec{k}_{\parallel}$  and the parallel magnetic field  $B_{\parallel}$ , respectively. Here,  $m^*$  and  $2a$  are the same as Fig. 1, the barrier separating the wells has width  $b = 20$  Å, and the middle barrier height is  $U_0 = 213$  meV. Figure 2(a) is a plot of the  $k_y$  dispersion for a fixed, large magnetic field  $B_{\parallel} = 10$  T. In Fig. 2(b), we set  $\vec{k}_{\parallel} = 0$ . The energy diagram in Fig. 2(a) shows that the quadratic energy dispersions of electrons in each of the pair of quantum wells anticross due to the in-plane magnetic field as well as the tunneling between the wells. This will produce minigaps and saddle points in the total density of states when  $B_{\parallel}$  is strong. The plot of the energy eigenvalues as a function of  $B_{\parallel}$  in Fig. 2(b) shows the splitting of the originally degenerate Landau energy levels due to tunneling in the strong magnetic field limit.

#### IV. PARTIAL DENSITY OF STATES FOR A SINGLE- AND DOUBLE-QUANTUM-WELL STRUCTURE IN A PARALLEL MAGNETIC FIELD

The single-particle Green's function that includes scattering by impurities is given by

$$G_{j\vec{k}_{\parallel}}(E) = \frac{1}{Z_{jk_y}(E) - \hbar^2 k_z^2 / 2m^*}, \quad (10)$$

where the scattering self-energy from impurities can be calculated in the self-consistent Born approximation

$$\begin{aligned} Z_{jk_y}(E) = E - E_j(k_y) + \frac{\sqrt{m^*}}{\hbar} \sum_{j'} \int_{-\infty}^{\infty} dk'_y \Gamma_{jk_y, j'k'_y} \\ \times \{ \sqrt{|Z_{j'k'_y}(E)| + \text{Re}Z_{j'k'_y}(E)} \\ + i \sqrt{|Z_{j'k'_y}(E)| - \text{Re}Z_{j'k'_y}(E)} \}^{-1}, \end{aligned} \quad (11)$$

with the impurity interaction vertex given by

$$\Gamma_{jk_y, j'k'_y} = \sum_n N_{\text{im}}^{2\text{D}}(n) [U_{jk_y, j'k'_y}^{\text{im}}(x_n)]^2. \quad (12)$$

In this notation,  $N_{\text{im}}^{2\text{D}}(n)$  stands for the  $n$ th sheet density of  $\delta$  doping, and the impurity interaction matrix element is defined as

$$U_{jk_y, j'k'_y}^{\text{im}}(x_n) = -\frac{e^2}{2\epsilon_0\epsilon_b} \int_{-\infty}^{\infty} dx \phi_{jk_y}(\xi_{k_y}) |x - x_n| \phi_{j'k'_y}(\xi_{k'_y}), \quad (13)$$

with  $x_n$  denoting the position of the  $n$ th  $\delta$ -doping layer. The contribution from the term in Eq. (11) involving the impurity interaction matrix  $\Gamma_{jk_y, j'k'_y}$  increases with the magnetic field. Therefore, the self-consistency of the calculation for the density of states becomes more important in the high magnetic field regime. Solving Eq. (11) for  $Z_{jk_y}(E)$ , the partial density of states  $D_{j\vec{k}_{\parallel}}(E)$  can be calculated from the Green's function in Eq. (10) and we obtain

$$D_{j\vec{k}_{\parallel}}(E) = \frac{1}{\pi} \text{Im}G_{j\vec{k}_{\parallel}}(E) = -\frac{1}{\pi} \frac{\text{Im}Z_{jk_y}(E)}{|Z_{jk_y}(E) - \hbar^2 k_z^2 / 2m^*|^2}. \quad (14)$$

We now present numerical results for the partial density of states for a single QW and a DQW in a parallel magnetic field.

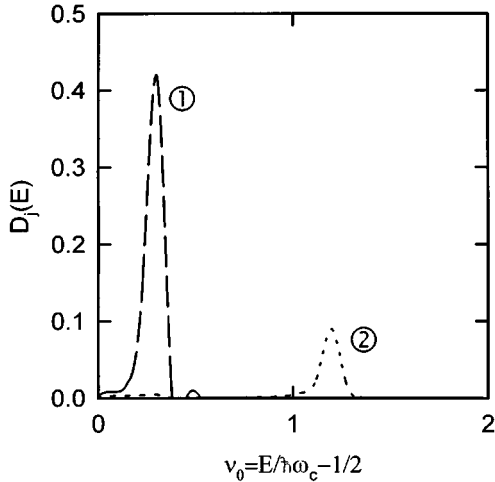


FIG. 3. The partial density of states  $D_{j\tilde{k}_y}(E)$  (per eV) for a DQW in a parallel magnetic field  $B_{\parallel}=10$  T and  $k_z=0$ . Here,  $m^*$ ,  $U_0$ ,  $a$ , and the barrier width between the two wells  $b$  are the same as Fig. 2. The barrier separating the wells is  $\delta$  doped at  $x_n=0$  with an impurity concentration of  $N_{\text{im}}^{2\text{D}}(n=0)=10^{11}$   $\text{cm}^{-2}$ . The in-plane wave vector is  $k_y=-\pi/a$ , for a half-well width  $a=100$  Å. The curve labeled “1” is for the lowest energy eigenvalue and “2” refers to the first excited state.

In Fig. 3, we have plotted the partial density of states in Eq. (14) for a pair of coupled QWs in a parallel magnetic field  $B_{\parallel}=10$  T. The parameters used for the well width and height  $U_0$  of the barriers on either side of the well are the same as those in Fig. 2. The sheet density for doping is  $N_{\text{im}}^{2\text{D}}(n=0)=10^{11}$   $\text{cm}^{-2}$  at  $x_n=0$  and the average background dielectric constant is  $\epsilon_b=11$ . For illustration, we present results for  $k_y=-\pi/a$ , where the half-width of the well is  $a=100$  Å and for the two lowest energy eigenvalues corresponding to this wave number. The broadening of the peaks for the self-consistent density of states was obtained by initializing the value of  $Z_{jk_y}(E) \approx E - E_j(k_y) + i\hbar/\tau$ , with the relaxation time parameter set as  $\tau=10^{-11}$  sec, and iterating Eq. (11) to convergence. Our results show that the line shape of the partial density of states  $D_{j\tilde{k}_y}(E)$  depends on both the index  $j$  of the energy eigenvalue for the specified wave number  $k_y$ .

## V. CONCLUDING REMARKS

In conclusion, we have derived the dispersion relation for the energy eigenvalues in a single-quantum-well and a DQW system in the presence of an in-plane magnetic field  $B_{\parallel}$ . For the double quantum well, the energy eigenvalues include tunneling between the quantum wells and subsequently display anticrossing features. The self-consistent Born approximation has been used to calculate the partial density of states. Our numerical results for the energy eigenvalues as a function of  $B_{\parallel}$  show a crossover behavior as the magnetic field is increased, at a critical magnetic field which corresponds to the well width being equal to the magnetic length. This means that for a pair of coupled quantum wells in a strong parallel magnetic field, the tunneling between the wells is suppressed in the high magnetic field limit so that

the electrons are confined to the wells. Our calculations for the wave functions support this conclusion. In the low magnetic field regime, the energy eigenvalue spectrum is more densely distributed compared to the high magnetic field region. In fact, the dimensionless energy eigenvalue spectra expressed in units of the cyclotron energy  $\hbar\omega_c$  are lines whose slopes become steeper as the magnetic field is lowered. When plotted as a function of the in-plane wave number  $k_y$ , the energy spectra for both the single- and double-quantum-well systems have gaps. The source of the gaps is due to the confining potential and, in the case of the double well structure, to the anticrossing of the energy dispersion in each well. The results for the energy eigenvalues are used to obtain the partial density of states as a function of the electron energy for fixed magnetic field strength. The role played by impurity scattering is included in the self-energy, in the self-consistent Born approximation. The magnitude of the contribution from the self-energy to the density of states increases with the magnetic field.

## ACKNOWLEDGMENTS

The authors gratefully acknowledge the support in part from the City University of New York PSC-CUNY-BHE Grant No. 666414.

## APPENDIX A

In this appendix, we present integral representations of the parabolic cylinder functions, solutions of Eq. (2), and list some of their properties. For arbitrary  $\nu$ ,  $V_\nu(x)$  can be expressed in terms of  $D_\nu(x)$  and  $D_\nu(-x)$  in the following way:<sup>17</sup>

$$V_\nu(x) = \frac{1}{\pi} \Gamma(-\nu) [D_\nu(-x) - \cos(\pi\nu) D_\nu(x)]. \quad (\text{A1})$$

When  $\nu$  is an integer  $D_\nu(-x) = (-1)^\nu D_\nu(x)$ ,

The integral representation of  $D_\nu(x)$  depends on the value of  $\nu$ . When  $\nu < 0$ , we have

$$D_\nu(x) = \frac{e^{-x^2/4}}{\Gamma(-\nu)} \int_0^\infty dt \exp\left(-xt - \frac{t^2}{2}\right) t^{-\nu-1}. \quad (\text{A2})$$

When  $\nu > -1$ , we have

$$\begin{aligned} D_\nu(x) &= \sqrt{\frac{2}{\pi}} e^{x^2/4} \int_0^\infty dt e^{-t^2/2} t^\nu \cos\left(xt - \frac{\pi\nu}{2}\right) \\ &\rightarrow x^\nu e^{-x^2/4} \left\{ 1 + \frac{\nu(1-\nu)}{2x^2} + \frac{\nu(\nu-2)(1-\nu)(3-\nu)}{8x^4} \right. \\ &\quad \left. + O\left(\frac{1}{x^6}\right) \right\}, \end{aligned} \quad (\text{A3})$$

as  $|x| \rightarrow \infty$ . We note that we have taken  $D_\nu(\xi_{k_y})$  and  $V_\nu(\xi_{k_y})$  as linearly independent solutions of Eq. (2). However, when  $\nu \neq 0, 1, 2, \dots$  another pair of linearly independent solutions is possible. These are  $D_\nu(\xi_{k_y})$  and

$D_\nu(-\xi_{k_y})$ , which are only linearly independent when  $\nu$  is not equal to a non-negative integer, but  $D_\nu(\xi_{k_y})$  and  $V\nu(\xi_{k_y})$  are linearly independent for arbitrary  $\nu$ . Therefore, if we are restricted to values of energy where  $\nu = E/\hbar\omega_c - 1/2$

$\neq 0, 1, 2, \dots$ , we can use  $D_\nu(-\xi_{k_y})$  instead of  $V\nu(\xi_{k_y})$  in the determinantal equations (2) and (9) determining the energy eigenvalues for the single-well and double-well problem, respectively.

\*Also at The Graduate School and University Center of the City University of New York, 33 West 42 Street, New York, NY 10036.

<sup>1</sup>J. P. Eisenstein, L. N. Pfeiffer, and K. W. West, Phys. Rev. Lett. **69**, 3804 (1992).

<sup>2</sup>K. M. Brown *et al.*, Phys. Rev. B **50**, 15 465 (1994); Appl. Phys. Lett. **64**, 1827 (1994).

<sup>3</sup>J. Smoliner *et al.*, Phys. Rev. Lett. **63**, 2116 (1989); J. P. Eisenstein *et al.*, Phys. Rev. B **44**, 6511 (1991); J. A. Simmons, S. K. Lyo, J. F. Klem, M. E. Sherwin, and J. R. Wendt, *ibid.* **47**, 15 741 (1993).

<sup>4</sup>A. Kurobe, I. M. Castleton, E. H. Linfield, M. P. Grimshaw, K. M. Brown, D. A. Ritchie, M. Pepper, and G. A. C. Jones, Phys. Rev. B **50**, 4889 (1994).

<sup>5</sup>G. S. Boebinger, A. Passner, L. N. Pfeiffer, and K. W. West, Phys. Rev. B **45**, 12 673 (1991).

<sup>6</sup>G. Aizin and G. Gumbs, Phys. Rev. B **52**, 1890 (1995).

<sup>7</sup>J. A. Simmons, S. K. Lyo, J. F. Klem, M. E. Sherwin, and J. R. Wendt, Phys. Rev. B **47**, 15 741 (1993).

<sup>8</sup>J. A. Simmons, S. K. Lyo, N. E. Harff, and J. F. Klem, Phys. Rev. Lett. **73**, 2256 (1994).

<sup>9</sup>S. K. Lyo and J. A. Simmons, J. Phys. Condens. Matter **5**, L299 (1993).

<sup>10</sup>S. K. Lyo, Phys. Rev. B **50**, 4965 (1995).

<sup>11</sup>S. K. Lyo, Phys. Rev. B **51**, 11 160 (1995).

<sup>12</sup>T. Jungwirth and L. Smrcka, J. Phys. Condens. Matter **5**, L217 (1993).

<sup>13</sup>W. Demmerle, J. Smoliner, G. Berthold, E. Gornik, G. Weimann, and W. Schlapp, Phys. Rev. B **44**, 3090 (1991).

<sup>14</sup>J. P. Eisenstein, L. N. Pfeiffer, and K. W. West, Appl. Phys. Lett. **58**, 1497 (1991).

<sup>15</sup>G. Rainer, J. Smoliner, E. Gornik, G. Böhm, and G. Weimann, Phys. Rev. B **51**, 17 642 (1995).

<sup>16</sup>A. Erdélyi, *Higher Transcendental Functions* (Krieger, Florida, 1981), Vol. II, p. 122.

<sup>17</sup>*Handbook of Mathematical Functions*, edited by M. Abramowitz and I. A. Stegun (Dover, New York, 1970), p. 685.